

# ADVANCED TOKAMAK BURNING PLASMA EXPERIMENT\*

M. PORKOLAB, P.T.BONOLI, J RAMOS, J. SCHULTZ

MIT Plasma Science and Fusion Center

Cambridge, Massachusetts 02139, USA

W.N. NEVINS

Lawrence Livermore National Laboratory

PO Box 808 (L-637)

Livermore, CA 94551, USA

## Abstract

A new reduced size ITER-RC superconducting tokamak concept is proposed with the goals of studying burn physics either in an inductively driven standard tokamak (ST) mode of operation, or in a quasi-steady state advanced tokamak (AT) mode sustained by non-inductive means. This is achieved by reducing the radiation shield thickness protecting the superconducting magnet by 0.34 m relative to ITER and limiting the burn mode of operation to pulse lengths as allowed by the TF coil warming up to the current sharing temperature. High gain ( $Q \simeq 10$ ) burn physics studies in a reversed shear equilibrium, sustained by RF and NBI current drive techniques, may be obtained.

## 1. INTRODUCTION AND OVERVIEW

We have examined the concept of a long pulse, optimized burning plasma experiment in a steady state tokamak facility operating with superconducting magnets. Based on physics and engineering scoping studies, we have found an attractive machine concept, with major radius of 5.60 m, magnetic fields above 6.0 T, and currents in the range of 12 -15 MA with pulse lengths up to 300 sec. The engineering design and ohmic performance of such a device has been presented recently [1]. Such a device would achieve  $Q \geq 10$  with conventional ITER confinement scaling as well as with advanced tokamak (AT) physics rules in the driven mode. An ATBX class device should cost no more than 50% of ITER. The substantial size reduction in ATBX is achieved by reducing the shielding on the inner wall of the vessel as compared to the canonical 1.2 m thickness required in a steady state burning plasma device, such as ITER or ITER-RC. The increased neutron flux associated with the reduced shielding results in an adiabatic temperature rise of the toroidal field winding. The pulse duration is limited so that the superconductor remains below the quench temperature to give adequate margin against plasma disruptions. Taking advantage of the steady state nature of the superconducting coils, the machine can be operated for long pulse (300 sec) or steady state with ITER-sized refrigeration unit.

To assure AT operation with high-bootstrap fraction ( $\approx 70\%$ ), adequate  $\beta$  ( $\gtrsim 3\%$ ) and high plasma current, we have kept the aspect ratio,  $R/a$  in the range of 3.0-3.2. It has been shown recently [2] that at such aspect ratios and sufficiently high elongation ( $\kappa_{95} = 1.8$ ) and triangularity ( $\delta_{95} \geq 0.4$ ), a  $\beta_N$  of order 3 is achievable in a stable manner with reversed shear, even without a conducting "smart" wall. We shall present results of modeling here by the ACCOME and PEST II-codes demonstrating that such an operating regime is achievable in ATBX with off-axis lower hybrid current drive and central negative ion beam or fast wave current drive. A neutron wall-loading of  $1\text{MW}/\text{m}^2$  is attained with the above parameters. Higher  $\beta_N$  (and therefore higher bootstrap fraction) operation is feasible by adding a conducting wall.

## 2. ILLUSTRATIVE DESIGN POINT IN ATBX

A spreadsheet was developed for sizing tokamak performance using the above approach for reducing the shielding thickness. A number of design points were studied and trends were plotted. The spreadsheet uses the 1990 ITER information document, updated to present ITER confinement scaling rules. The spreadsheet was benchmarked using the current ITER design. The concept takes advantage of the heat capacity of the coil and helium in determining the time for the coil to warm up to the current sharing temperature, the actual critical temperature of the superconductor being a key parameter. It is expected that a substantial fusion power can be tolerated and that even full-power steady-state operation is possible with increased refrigeration. Assuming inductive current drive and central auxiliary heating, engineering studies have been carried out recently [1], and burn times of order of 300 seconds have been obtained. Table I exhibits an operating point at a density well below (by  $\sim 30\%$ ) the Greenwald limit (at  $n \simeq n_{GW}$ ,  $Q \approx 40!$ )

**TABLE I.**  
ATBX PARAMETERS WITH OHMIC OPERATION

Major radius (m):	5.60	$q_{95}$	3.5
Minor radius (m)	1.75	Fusion power (MW)	690
Total flux capability (Vs)	291	$\tau_E$ (s) ( $0.81 \times$ ITER93H-ELM-free)	2.2
Aspect ratio(A)	3.2	$P_{aux}$ (MW)	74
$\kappa_{95}$	1.8	Warm shield thickness (m)	0.58
$\delta_{95}$	0.4	Flat top flux capability (Vs)	28.9
B (T)	6.25	$Q_{DT}$	9.3
Plasma current (MA)	14.7	Neutron wall load (MW/m <sup>2</sup> )	1.0

### 3. PARAMETRIC STUDY OF MHD STABILITY LIMITS IN THE ADVANCED TOKAMAK REGIME

To determine the “optimal” parameters for an AT tokamak, first we have undertaken a systematic MHD stability analysis of different reversed shear (or negative central shear, NCS) equilibria, with the aim of identifying the dependence of the stability limits on parameters that have a significant impact on the machine design. Specifically we have considered the effects of the aspect ratio ( $A = R/a$ ), the triangularity ( $\delta$ ) and the plasma current ( $I_p$ ). The advanced tokamak regime of interest corresponds to high values of the poloidal beta, and minimum values of the safety factor  $q_{min}$  above 2, so that it is possible to access the ballooning second stability region and to generate a large fraction of bootstrap current. For the geometry of the plasma boundary we adopt a conventional up-down symmetric D-shape of constant elongation  $\kappa = 1.8$ , while the aspect ratio and the triangularity are varied. Based on past theoretical studies, a nearly optimum equilibrium is achieved for central and minimum values of the safety factor,  $q_0 = 3.5$ ,  $q_{min} = 2.2$ , respectively, with the position of such minimum being at  $r/a=0.7$ . The stability limits are very sensitive to  $q_{min}$  and the threshold for the n=1 mode drops significantly ( $\sim 20\%$ ) if  $q_{min}$  approaches an integer from below. The choice  $q_{min} = 2.2$  was found previously to be near optimal [2]. For the pressure profile we keep a constant functional form,  $p_\psi/p_0 = (1 - \psi)^2$ , where  $\psi$  is the normalized poloidal flux and  $p_0$  is varied to scan different plasma betas. This profile results in values of the ratio of the peak to the volume averaged pressure between 2.6 and 2.8. Finally, for the purpose of comparing the bootstrap current figure of merit in the different equilibria, the bootstrap fraction  $f_{bs}$  is computed for fixed temperature and density profiles  $T(\psi)/T(0)=(1-\psi)^{1.5}$ ,  $n(\psi)/n(0)=(1 - \psi)^{0.5}$ . The above described equilibria are always ballooning stable, with access to the second stability region. Their ideal MHD stability limit is set by the n=1 external mode in the absence of a conducting wall. These stability limits, obtained numerically with the J-SOLVER and PEST-II codes, are summarized in Tables II and III.

Table II shows the marginal stability parameters at a constant triangularity  $\delta = 0.4$ , and two different values of the aspect ratio,  $A=4.0$  and  $3.0$ . Shown are different values of the normalized current  $I/aB$ ,  $AI/aB$  and the edge safety factor  $q_a$ . Note that significantly higher values of  $\beta$  are obtained at  $A=3.0$  for nearly the same bootstrap current fraction as at  $A=4.0$ . We see that for reasonably high values of the bootstrap fraction,  $\beta$  increases from 2.0% to 3.1% for  $q_a = 6.1$ , and from 2.4% to 3.9% for  $q_a=4.0$ , respectively, as the aspect ratio is lowered from 4.0 to 3.0. Table III shows the marginal stability parameters for a constant aspect ratio  $A=3.0$ , and three values of the triangularity,  $\delta$ . Notice that we have carried out comparisons at constant  $AI/aB$  and constant  $q_a$  independently, since these two parameters are not equivalent in toroidal geometry. The bootstrap fractions accompanied by a \* correspond to equilibria where the bootstrap current profile equals the total equilibrium current profile at some radial location. When \*\* appears in the bootstrap fraction field, the bootstrap current exceeds the equilibrium current somewhere and a negative external current drive would be necessary (such as provided by a realistic lower-hybrid wave launching spectrum).

**TABLE II**  
ASPECT RATIO (A=R/a) SCALING OF  $\beta$  LIMITS AT  $\delta = 0.4$

	<b>A=4.0</b>	<b>A=4.0</b>	<b>A=3.0</b>	<b>A=4.0</b>	<b>A=4.0</b>	<b>A=3.0</b>
A I(MA)/a(m) B(T)	4.0	3.72	4.0	3.0	2.83	3.0
I/aB	1.0	0.93	1.33	0.75	0.71	1.0
$q_a$	3.5	<b>4.0</b>	<b>4.0</b>	5.5	<b>6.1</b>	<b>6.1</b>
$\beta_N$	1.75	2.6	2.9	2.7	2.8	3.1
$\beta$	1.75%	2.4%	3.9%	2.0%	2.0%	3.1%
$f_{bs}$	0.36	0.54	0.50	0.61*	**	0.60*

A further optimization of the bootstrap fraction can be achieved by modifying the temperature and density profiles while keeping their product, i.e. the pressure profile, invariant so that the above MHD stability results do not change. After this, and for the optimal geometrical parameters A=3.0,  $\delta = 0.5$ , we find stable equilibria with  $\beta_N = 3.0$ ,  $\beta = 2.8\%$  and  $f_{bs} = 0.75$  at I/aB=0.94 MA/mT and  $q_a = 7.4$ , or  $\beta_N = 3.1$ ,  $\beta = 3.4\%$  and  $f_{bs} = 0.70$  at I/aB=1.09 MA/mT and  $q_a = 6.1$ . This last case represents the “optimized” geometry we will use in our design of ATBX. Extensive studies such as presented above indicate the following: (i) increasing the edge  $q_a$  would increase  $\beta_N$  and the bootstrap fraction (but would reduce confinement through its dependence on  $I_p$ ); (ii) lowering  $\delta_{95}$  below 0.35, or peaking the pressure profile above 3, deteriorates stability (lowers the stable range of  $\beta_N$ ) without a conducting wall; (iii) increasing the aspect ratio, A will lower beta (for  $\beta_N$  being near the stability limit); (iv) a conducting wall is necessary for  $\beta_N \gtrsim 3.5$ ,  $f_{bs} \gtrsim 0.75$ ,  $q_{95} \lesssim 5$ .

**TABLE III**  
COMPARISON OF  $\beta$  LIMITS AT A = 3.0

	<u><math>\delta = 0.3</math></u>	<u><math>\delta = 0.3</math></u>	<u><math>\delta = 0.4</math></u>	<u><math>\delta = 0.5</math></u>	<u><math>\delta = 0.5</math></u>	<u><math>\delta = 0.5</math></u>
AI/a B	2.82	3.0	3.0	3.27	3.0	2.65
I/aB	0.94	1.0	1.0	1.09	1.0	0.88
$q_a$	6.1	5.5	6.1	6.1	7.0	8.7
$\beta_N$	2.95	2.85	3.1	3.1	3.2	3.2
$\beta$	2.80%	2.85%	3.1%	3.4%	3.2%	2.8%
$f_{bs}$	**	0.56	0.60*	0.57	0.61*	**

#### 4. REVERSED SHEAR ADVANCED TOKAMAK REGIME IN ATBX

Self-consistent equilibria in ATBX was developed with the ACCOME code [2] and stability analysis was carried out with the PEST-II code. The target plasma was maintained by means of off-axis lower-hybrid current drive, central neutral beam current drive and/or fast wave current drive. The MHD equilibria and current density profiles from ACCOME were coupled to the JSOLVER/PEST [2] equilibrium and stability package. Thus the current profile control results from ACCOME could be tested for stability to the  $n = \infty$  ballooning mode and the low  $n = (1,2,3)$  external kink modes. The results of the ACCOME Code simulation are show in Table IV. The equilibrium is obtained with 60 MW of lower-hybrid power at a frequency of 5.5 GHz and 20 MW of NBI at 500 keV peak energy. The launched LH spectrum peaks at  $N_{\parallel} = 1.90$ . The negative part of the spectrum is included, and it drives negative edge currents which tends to cancel the edge bootstrap current and improves stability. The bootstrap fraction is 71% at a stable equilibrium with  $\beta_N = 2.8$ . The total plasma current is 12 MA. The stability analysis show that the plasma is stable to  $n = 1,2,3$  kink modes and ballooning modes. The  $\alpha$  particle pressure is included in these calculations. Adding a conducting wall at  $r/a = 1.3$  provides stability up to  $\beta_N \simeq 5$  and  $f_{bs} \sim 90\%$  (approaching the ARIES-RS plasma parameters). The current and  $q$ -profiles are shown in Figs. 1,2. The EXCEL spreadsheet predicts that the fusion power output is 845 MW, or  $Q_{DT} = 10.5$ , with a confinement of  $\tau_E \simeq 2.0$  sec and  $\tau_E/\tau_{ITER98H} = 1.3$  (corresponding to H=2.5 relative to ITER89-L mode scaling). This value is quite conservative

for an AT scenario where one would expect  $H_{89-P} > 3$ . The wall loading is  $1.2 \text{ MW/m}^2$ , and the total power ( $P_{aux} + P_{\alpha} = 212 \text{ MW}$ ) exceeds the required H-mode threshold power (180 MW) at full operating density. We note that at the operating point we remain well below the Greenwald density limit.

---

**TABLE IV**  
ACCOMME RESULTS OF ATBX REVERSED SHEAR EQUILIBRIUM

---

**PROFILES:**

$$p(\psi) = n(\psi)T(\psi) = p_o(1 - \psi)^2; \quad T(\psi) = T_0/[0.70(1 - \psi)^{1.5} + 0.30(1 - \psi^4)]$$

$n_{e0} = 2.00 \times 10^{20} \text{m}^{-3}$	$\kappa_{95} = 1.85$	$\beta_t = 2.91\%$
$\langle n_e \rangle = 0.983 \times 10^{20} \text{m}^{-3}$	$\delta_{95} = 0.44$	$\beta_p = 1.64$
$T_{e0} = 22.0 \text{ keV}$	$q_0 = 4.0$	$\beta_N = 2.79$
$\langle T_e \rangle_n = 16.07 \text{ keV}$	$q_{min} = 2.5$	$I_{NBI} = 0.96 \text{ MA}$
$T_{d0} = 22.0 \text{ keV}$	$q_{95} = 5.0$	$I_{LH} = 2.49 \text{ MA}$
$\langle T_d \rangle_n = 16.07 \text{ keV}$	$\ell_i = 0.58$	$I_{bs} = 8.53 \text{ MA}$
$p_0/\langle p \rangle = 2.8$	$I_p = 11.98 \text{ MA}$	$f_{bs} = I_{bs}/I_p = 0.71$

---

**SUMMARY**

In conclusion, a new superconducting tokamak concept has been proposed which would have the twin goals of studying steady state AT physics, while allowing burn physics studies, including the impact of helium ash accumulation. This is achieved by reducing the radiation shield thickness by 0.34 m and limiting the burn mode of operation to pulse lengths as allowed by the TF coil warming up to the current sharing temperature. Marrying the AT and ST modes of operation would allow optimized high gain burn physics studies in ATBX.

\* Work supported by US DOE Contract DE-FC02-93ER54186.

**REFERENCES**

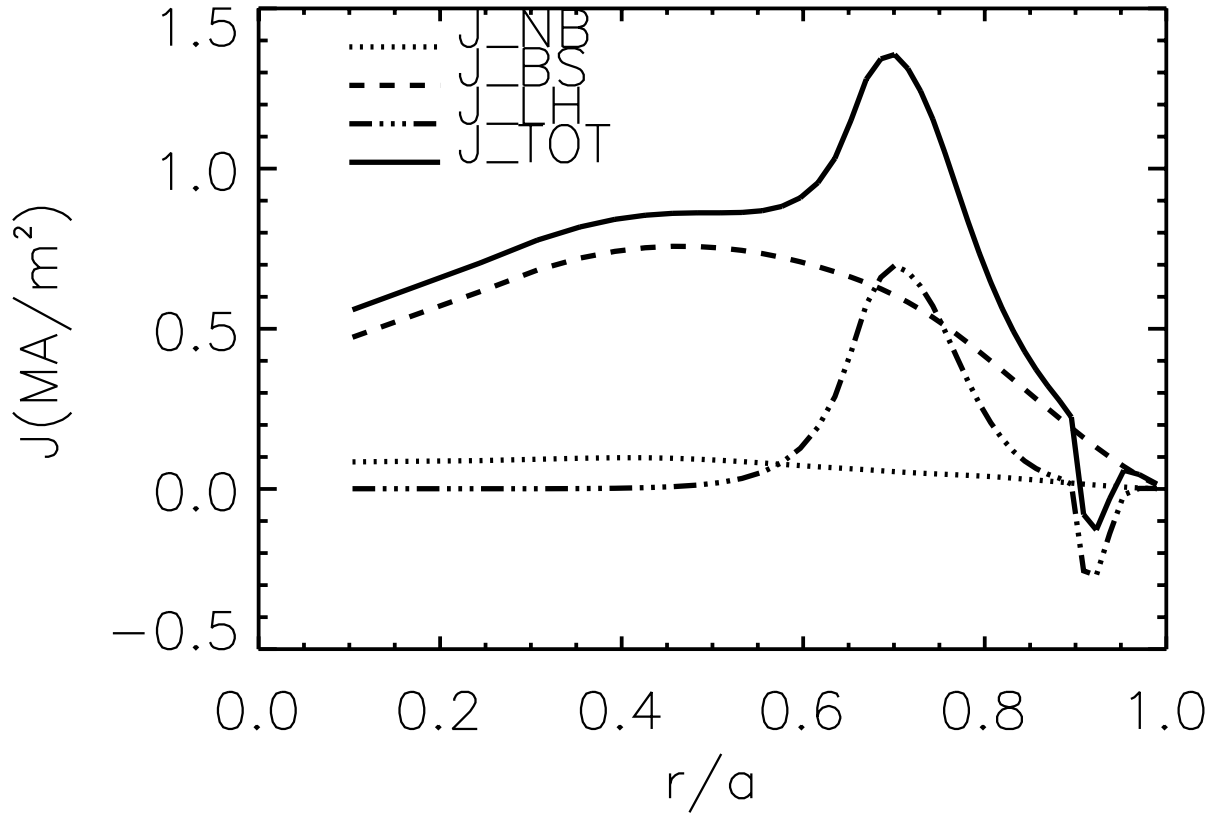
- [1] J.H. SCHULTZ, M. PORKOLAB, P. TITUS, P. HEITZENROEDER, C. KESSEL, J. SCHMIDT, T. BROWN, AND M. SAWAN, III Applied Superconductivity Conf., Palm Desert, CA, Sept 14, 1998 (to be published).
- [2] P.T. BONOLI, M. PORKOLAB, J. RAMOS, W. NEVINS AND C. KESSEL, Plasma Phys. Contr. Fusion **39**, (1997) 22; See also references therein.

**FIGURES**

Figure 1: Current density profiles

Figure 2: q profile

# Current Density Profiles



# Q-PROFILE

